



**1ST INTERNATIONAL CONFERENCE ON PHONONIC CRYSTALS,  
METAMATERIALS & OPTOMECHANICS**

**Extended Abstracts**

**Track 7: Phononic MEMS and RF Applications**

Phononics 2011: First International Conference on Phononic Crystals, Metamaterials and Optomechanics

Santa Fe, New Mexico, USA, May 29-June 2, 2011

PHONONICS-2011-0053

## Tunable magnetoelastic phononic crystals

J.O. Vasseur<sup>1</sup>, O. Bou-Matar<sup>1</sup>, J-F. Robillard<sup>1</sup>, A.-C. Hladky-Hennion<sup>1</sup>, and P.A. Deymier<sup>2</sup>

<sup>1</sup> *Institut d'Électronique, de Microélectronique et de Nanotechnologie, UMR CNRS 8520, Cité Scientifique, 59652 Villeneuve d'Ascq Cedex, France,*

*Jerome.Vasseur@univ-lille1.fr, olivier.boumatar@iemn.univ-lille1.fr, jean-francois.robillard@isen.fr, anne-christine.hladky@isen.fr*

<sup>2</sup> *Department of Materials Science and Engineering, University of Arizona, Tucson, Arizona 85721, USA deymier@email.arizona.edu*

**Abstract:** The feasibility of contactless tunability of the band structure of two-dimensional phononic crystals is demonstrated by employing magnetostrictive materials and applying an external magnetic field. The influence of the amplitude and of the orientation with respect to the inclusion axis of the applied magnetic field are studied in details. Applications to tunable selective frequency filters are discussed.

Phononic crystals may have potential applications in numerous technological domains [1]. Nevertheless, one of the major stumbling block to the application of phononic crystals is the lack of practical frequency tunability of their properties. Tunability could be achieved by changing the geometry of the inclusions [2] or by varying the elastic characteristics of the constitutive materials through application of external stimuli [3]. For instance, some authors have proposed the use of electrorheological materials in conjunction with application of external electric field [4]. Other authors have considered the effect of temperature on the elastic moduli [5]. In all cases, significant effect on the band structure of the phononic crystal can only be achieved by applying stimuli with very large magnitude. Recent work [6] exploits the change of the structure of the phononic crystal due to an external stress to alter the band structure. However this approach requires physical contact with the phononic crystal. We propose a contactless way to tune the properties of phononic crystals using magnetoelastic components. The elastic properties of a magnetoelastic material are very sensitive to its magnetic state and on the applied external magnetic field. For instance, in giant magnetostrictive material, such as Terfenol-D, this dependence can lead to more than 50% variation of some of the elastic constants, even at ultrasonic frequencies [7]. Moreover, for some directions of the applied external magnetic field, a spin reorientation transition (SRT) appears leading to even more variations of the elastic constants. So, if one of the components of a phononic crystal is a magneto-elastic medium, then one can expect that the elastic contrast, and subsequently the phononic crystal properties could be controlled without any contact by a magnetic field.

We studied in details the tuning of the properties of a bulk two-dimensional magnetoelastic phononic crystal when an external magnetic field is applied. We developed first a theoretical model allowing to derive for an arbitrary direction and amplitude of the applied magnetic field, an equivalent piezomagnetic material of a polarized ferromagnet, with field dependent elastic  $C_{ijkl}$ , piezomagnetic  $q_{ij}$  and magnetic permeability  $\mu_{ij}$  constants. For example, Figure 1 presents the variations of these constants as functions of the applied magnetic field in the case of an infinite Terfenol square rod and for a magnetic field parallel to the direction of the rod. One observes that some of these constants strongly depend on the magnetic field amplitude. Using the equivalent constants, we computed the band structures of two-dimensional arrays of Terfenol-D square rods embedded in an epoxy matrix with the help of the well-known Plane Wave Expansion (PWE) method [8]. The band structures of Figs. 2(b) and 2(c) illustrate the effect of the external magnetic field. In absence of an external stimulus, the phononic crystal possesses two absolute band gaps ranging from approximately 0.5 to 0.8 MHz and from 0.89 to 1 MHz. Application of a magnetic field parallel to the Terfenol-D rods with a magnitude of 13 kOe enlarges the first band gap from 0.5 to 0.92 MHz and closes the second band gap. This shows that this phononic crystal behaves like a tunable filter with switching functionality for frequencies around 1 MHz.

Phononics 2011: First International Conference on Phononic Crystals, Metamaterials and Optomechanics

Santa Fe, New Mexico, USA, May 29-June 2, 2011

PHONONICS-2011-0053

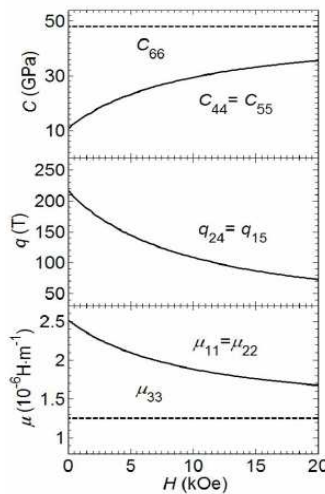


**Figure 1:** Evolution of the effective elastic moduli, piezomagnetic constants, and magnetic permeabilities of a Terfenol-D rod as a function of the static external magnetic field applied along the rod axis. The effective elastic and piezomagnetic constants are expressed in Voigt notation.

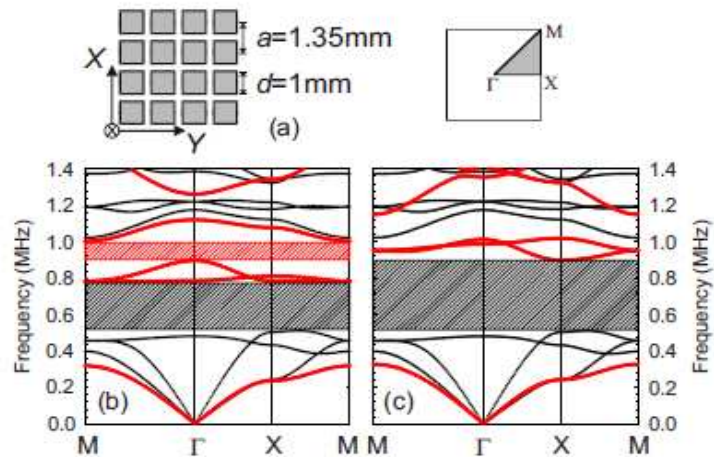


**Figure 2:** (a) The square-lattice 2D phononic crystal consisting of magneto-elastic square rods of infinite length along the  $Z$  direction made of Terfenol-D and embedded in an epoxy matrix. Band structure of a square lattice of Terfenol-D square rods with a filling factor  $f=(d/a)^2=0.55$ , embedded in an epoxy matrix for two applied static magnetic fields: (b)  $H_{\text{ext}}=0$  kOe and (c)  $H_{\text{ext}}=13$  kOe. The inset shows the irreducible Brillouin zone of the square array.

We will discuss the effect of the magnitude and of the orientation of the magnetic field on the band structure of the phononic crystal.

The introduction of a magnetoelastic constituent opens the possibility of easy controllability of the properties of a phononic crystal without any contact. Using this controllability, one may imagine to design devices with tunable functionalities such as frequency filters, superlens for acoustic imaging, etc... Some of these possible applications will be presented during this talk.

## References

- <sup>1</sup> Y. Pennec, J. O. Vasseur, B. Djafari-Rouhani, L. Dobrzynski, P. A. Deymier, *Surf. Sci. Reports* **65**, 229 (2010).
- <sup>2</sup> C. Goffaux and J. Vigneron, *Phys. Rev. B* **64**, 075118 (2001).
- <sup>3</sup> J. Baumgartl, M. Zvyagolskaya, and C. Bechinger, *Phys. Rev. Lett.* **99**, 205503 (2007).
- <sup>4</sup> J.-Y. Yeh, *Physica B* **400**, 137 (2007).
- <sup>5</sup> Z.-G. Huang and T.-T. Wu, *IEEE Trans. Ultrason. Ferroelectr. Freq. Control* **52**, 365 (2005).
- <sup>6</sup> K. Bertoldi and M. Boyce, *Phys. Rev. B* **77**, 052105 (2008).
- <sup>7</sup> Y. Wang, F. Li, Y. Wang, K. Kishimoto, and W. Huang, *Acta Mecha. Sinica* **25**, 65 (2009).
- <sup>8</sup> J. Cullen, S. Rinaldi, and G. Blessing, *J. Appl. Phys.* **49**, 1960 (1978).
- <sup>9</sup> J.-F. Robillard, O. Bou Matar, J. O. Vasseur, P. A. Deymier, M. Stippinger, A.-C. Hladky-Hennion, Y. Pennec and B. Djafari-Rouhani, *App. Phys. Lett.* **95**, 124104 (2009).

Phononics 2011: First International Conference on Phononic Crystals, Metamaterials and Optomechanics

Santa Fe, New Mexico, USA, May 29-June 2, 2011

PHONONICS-2011-0054

## Band Gaps and Defect Modes in Phononic Strip Waveguides

**Y. Pennec<sup>1</sup>, C. Li<sup>1</sup>, Y. El Hassouani<sup>1</sup>, J. M. Escalante<sup>2</sup>, A. Martinez<sup>2</sup>, B. Djafari Rouhani<sup>1</sup>**

<sup>1</sup> Institut d'Electronique, de Microélectronique et de Nanotechnologies, UMR CNRS 8520, Université de Lille1, Avenue Poincaré, Cité Scientifique, 59652 Villeneuve d'Ascq, France

yan.pennec@univ-lille1.fr

<sup>2</sup> Nanophotonics Technology Center, Universidad Politécnica de Valencia, Camino de Vera s/n 46022, Spain

**Abstract:** We study the elastic wave propagation in different geometries of strip waveguides obtained by extracting a row out of a phononic crystal slab made up of a square array of air holes in a silicon plate. We show that the existence of band gaps is strongly dependent on the cutting direction. We also study the existence of localized modes in cavities inserted inside the perfect strip waveguides.

We investigate the existence of band gaps in three kinds of phononic strip waveguides obtained by extracting a row in a phononic crystal slab constituted by a periodic array of air holes in a silicon plate. Figure 1 displays the three structures when the slab is cut along  $[1,0]$  and  $[1,1]$  directions. The band structures are calculated mostly by the finite element method using COMSOL Multiphysics. For each cutting direction, we discuss the existence and the behavior of band gaps as a function of the reduced geometrical parameters  $r/a$  and  $h/a$  where 'r' represents the radius of the holes, 'h' the thickness of the plate and 'a' the lattice parameter. Then, we have investigated the possibility of confined modes inside cavities inserted in the phononic strip waveguide. Figure 2 illustrates the example of a defect cavity obtained by reducing the radius of one hole from  $r/a=0.3$  in the perfect structure to  $r/a=0.2$ . Using a super-cell to calculate the band structure of the waveguide with the defect, one can observe the existence of a flat branch in the band gap. The map of the displacement field at the frequency of the flat band shows a localization of the mode in the cavity around the defect hole.

Currently, we are investigating the design of strip waveguides that allow dual phononic and photonic band gap, simultaneous confinement of both elastic and electromagnetic waves in cavities, and the possibility of single guided mode which presents a slow light and/or sound velocity.

**Acknowledgments:** This work was supported in part by the European Commission Seventh Framework Programs (FP7) under the FET-Open project TAILPHOX N° 233883 and IP project NANO-PACK N° 216716.

Figure 1

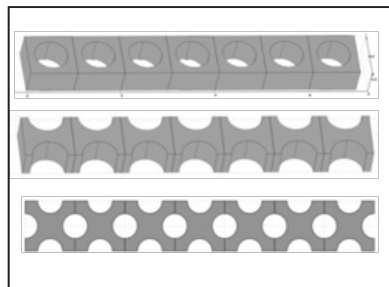
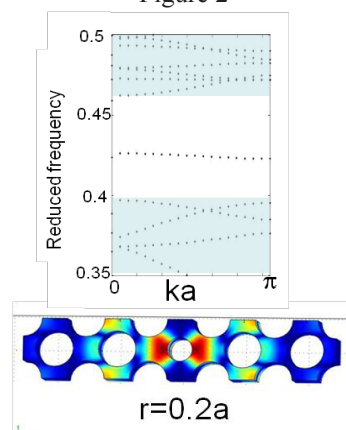


Figure 2



Phononics 2011: First International Conference on Phononic Crystals, Metamaterials and Optomechanics

Santa Fe, New Mexico, USA, May 29-June 2, 2011

PHONONICS-2011-0054

Phononics 2011: First International Conference on Phononic Crystals, Metamaterials and Optomechanics

Santa Fe, New Mexico, USA, May 29-June 2, 2011

PHONONICS-2011-0070

## Multi-phonon Processes in PhoXonic Cavities

**I.E. Psarobas<sup>1,2</sup>, N. Papanikolaou<sup>2</sup>, N. Stefanou<sup>1</sup>**

<sup>1</sup> Section of Solid State Physics, University of Athens, Panepistimioupolis, 15784, Athens, Greece, [ipsarob@phys.uoa.gr](mailto:ipsarob@phys.uoa.gr), [nstefan@phys.uoa.gr](mailto:nstefan@phys.uoa.gr)

<sup>2</sup> Institute of Microelectronics, NCSR "Demokritos", 15310, Athens, Greece  
[N.Papanikolaou@imel.demokritos.gr](mailto:N.Papanikolaou@imel.demokritos.gr)

**Abstract:** Long lifetime photons and phonons, confined in the same region of space, inside a phoXonic cavity, can interface with each other via strong nonlinear acousto-optic interactions. We unveil physics of distinct importance as the hypersonic modulation of light is substantially enhanced through multi-phonon exchange mechanisms.

Classical wave transport in periodic media can provide the means to control light, sound or both with the development of phoXonic crystals<sup>1</sup>, a special class of dual spectral-gap materials which can integrate the management of sound, heat and light in a versatile manner, although the manipulation of phonon states to achieve heat management is somewhat a more complicated issue. An example of a 3D phoXonic crystal with predicted dual functionality is given in Fig.1 after Ref. 1. Such structures are an essential step towards the hypersonic modulation of light and could lead to the development of efficient acousto-optical devices.

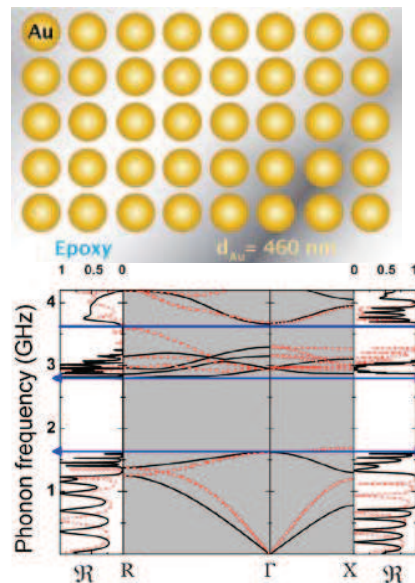


**Figure 1** A 3D metallodielectric phoXonic crystal of a simple cubic (*sc*) arrangement of gold nanospheres (460 nm in diameter) in epoxy. The lattice constant is 480 nm and the structure exhibits an absolute photonic spectral gap of 15%, around the telecom frequency. The absolute phononic gap is about 53% at the hypersonic frequency of 2 GHz. In the complex band structure diagrams along the *sc* symmetry points the corresponding omnidirectional gaps are marked with the double headed arrows. The corresponding reflection spectra for a slab of the crystal five layers thick is given along the (001) (right) and (111) (left) directions. The dotted reflection spectra corresponds to the case of surface reflection by a semi-infinite crystal. The complex permittivity of gold spheres is obtained from the experimental optical data found in Ref. 2.

Nevertheless, the physics of photon-phonon interaction inside a phoXonic structure, is still under serious investigation and can be summarized in two major categories, the optomechanics<sup>3</sup> and the acousto-optics<sup>4</sup>. The acousto-optic (AO) interaction realized in the merging fields of nanophotonics and nanophonics could lead to novel unprecedented control of light and sound in very small regions of space. In the regime of inelastic light scattering by sound, one can have phonon-assisted light emission, control of light speed (delay-storage) by stimulated Brillouin scattering and the realization of highly sensitive dual phoXonic sensors. In particular, phoXonic resonant cavities have the ability to enhance the acousto-optic interaction between localized photonic and phononic states in a Raman-Nath-like scattering pattern through multi-phonon exchange mechanisms. As an example, in Fig. 2 we present a model 1D resonant phoXonic cavity realized by Bragg mirrors consisting of homogeneous SiO<sub>2</sub> and Si multilayers. The time evolution of the

Phononics 2011: First International Conference on Phononic Crystals, Metamaterials and Optomechanics

Santa Fe, New Mexico, USA, May 29-June 2, 2011

PHONONICS-2011-0070

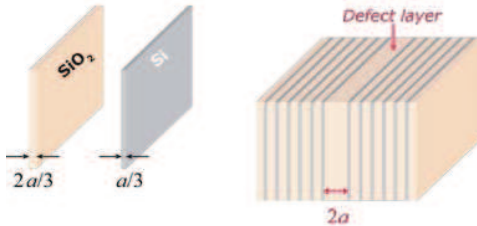


**Figure 2** A 1D phoXonic cavity consisting of homogeneous SiO<sub>2</sub> and Si layers with a SiO<sub>2</sub> layer in the middle. The structure has lattice constant  $a = 300$  nm.

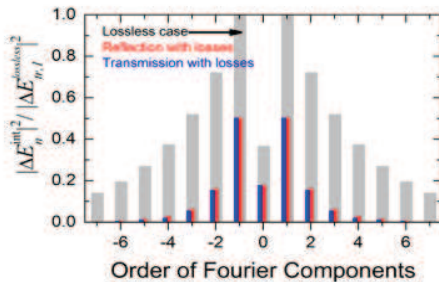


**Figure 3** Optical reflection-transmission through the phoXonic structure of Fig. 2 under a continuous acoustic excitation of input level  $u_0 = 0.1$  nm (at 10.9 GHz), for normally incident light at the resonance wavelength. The Fourier components of the AO interaction are normalized with respect to the first order component with a resonant acoustic excitation without losses.

Obviously the effect is somewhat diminished, as compared to the lossless acoustic case, when hypersonic attenuation is considered. Nevertheless, the assumption of a strong inelastic light scattering process is still valid<sup>4</sup>. Starting from the above Raman-Nath-like effect, we are going to present potential polymer phoXonic structures, as well as cases of phoXonic resonant cavities accommodating localized modes or zones of slow light and sound, in order to unveil interesting physics of distinct importance.

Finally, we note that all calculations were carried out by the layer-multiple-scattering (LMS) method<sup>5</sup>, which is well documented for both elastodynamics<sup>6</sup> and electrodynamics<sup>7</sup>. The theory provides a framework<sup>5</sup> for a unified description of wave propagation in 1-3D periodic structures, finite slabs of layered structures, and systems with impurities: isolated impurities, impurity aggregates, or randomly distributed impurities. Recently, we have extended its capability to cases of any axisymmetric scatterer, besides spheres. This powerful tool describes accurately the acoustic and the optical response of composite structures made of a number of different layers having the same 2D periodicity and computes a full complex band structure and the response (transmission, reflection, absorption) of finite and semi-infinite systems.

This work was financially supported by the EU FET- Open project TAILPHOX Grant No. 233883 (<http://www.tailphox.org>).

## References

- <sup>1</sup> N. Papanikolaou, I. E. Psarobas, and N. Stefanou, *Appl. Phys. Lett.* **96**, 231917 (2010).
- <sup>2</sup> P. B. Johnson and R. W. Christy, *Phys. Rev. B* **6**, 4370 (1972).
- <sup>3</sup> M. Eichenfield, J. Chan, R. M. Camacho, K. J. Vahala, and O. Painter, *Nature* **462**, 78 (2009).
- <sup>4</sup> I.E. Psarobas *et al.*, *Phys. Rev. B* **82**, 174303 (2010).
- <sup>5</sup> A. Modinos, N. Stefanou, I. E. Psarobas, and V. Yannopapas, *Physica B* **296**, 167 (2001).
- <sup>6</sup> R. Sainidou, N. Stefanou, I. E. Psarobas, and A. Modinos, *Comput. Phys. Commun.* **166**, 197 (2005).
- <sup>7</sup> N. Stefanou, V. Yannopapas, and A. Modinos, *Comput. Phys. Commun.* **132**, 189 (2000).

Phononics 2011: First International Conference on Phononic Crystals, Metamaterials and Optomechanics

Santa Fe, New Mexico, USA, May 29-June 2, 2011

PHONONICS-2011-0090

## Band-gap operating in the gigahertz frequencies for a bi-layer phononic crystal slab

A. Talbi, A. Soltani, Y. El Hassouani, Y. Pennec\*, B. Djafari-Rouhani and A. Akjouj

*Institut d'Electronique, de Microélectronique et de Nanotechnologie, CNRS UMR 8520, Université Lille Nord de France, Lille 1, 59655 Villeneuve d'Ascq, France*

\*yan.pennec@univ-lille1.fr

**Abstract:** We investigate a phononic slab composed by two different layers. The phononic crystal is obtained drilling the bi-layer phononic slab by air holes. We study the existence and the behavior of absolute band gaps in such membrane both in theory and experiment.

We investigate the possibility of designing phononic crystal-based devices for telecommunication applications using materials commonly employed in microfabrication. The phononic crystal is composed by an aluminum nitride (AlN) slab of thickness 2800nm deposited on a thin metallic membrane of titanium Nitride (TiN) of thickness 250nm. This original native bi-layer membrane has been chosen to avoid the fragility of the whole structure. The purpose of this presentation is to show that such a structure presents absolute band gaps and to study its behavior as a function of the geometrical parameters. This theoretical study is completed by an experimental evidence of the band gap.

As an example of the experimental work, the figure (a) shows a SEM micrograph of the manufactured square array phononic crystal structure. The lattice parameter is  $a=1\mu\text{m}$  and the radius of the holes is  $r=450\text{nm}$ , corresponding to the high filling factor  $\beta=64\%$ . The figure (b) corresponds to a measurement of the transmission spectrum through the bi-layer phononic slab which contained ten periods of the square lattice. The propagation corresponds to the principal direction  $\Gamma X$  of the Brillouin zone. As seen in the normalized transmission spectrum, we have obtained a band gap closed to 1 GHz. The measured results are in good agreement with the theoretical predictions (not shown here) which lead to an absolute band gap in the same frequency range.

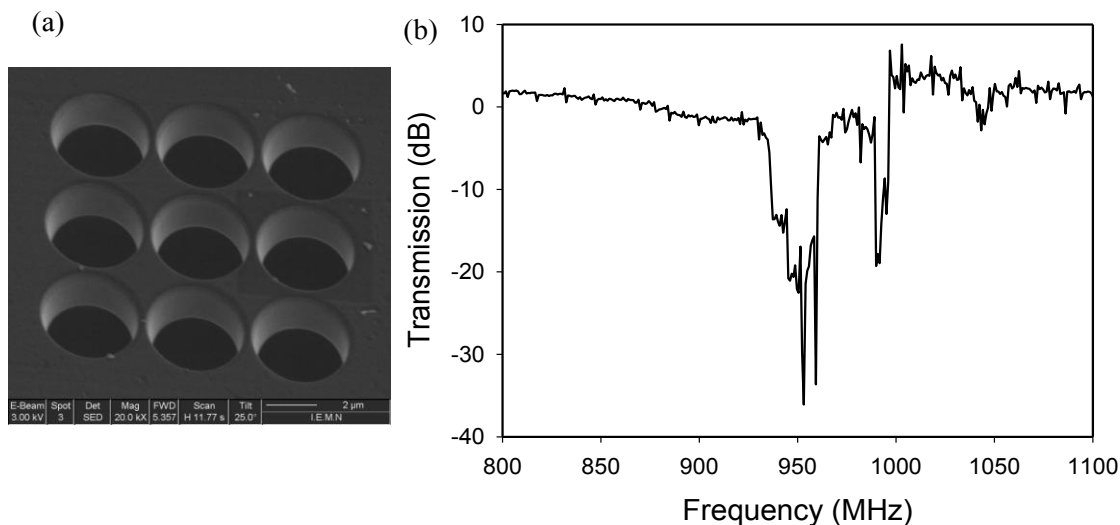


Figure: (a) Top view of one of the fabricated devices with the square lattice phononic structure. (b) Normalized average transmission measured through the phononic slab structure shown in Fig. (a) as a function of frequency. The figure presents one absolute band gaps in the GHz frequency range.

Phononics 2011: First International Conference on Phononic Crystals, Metamaterials and Optomechanics

Santa Fe, New Mexico, USA, May 29-June 2, 2011

PHONONICS-2011-0090

Phononics 2011: First International Conference on Phononic Crystals, Metamaterials and Optomechanics

Santa Fe, New Mexico, USA, May 29-June 2, 2011

PHONONICS-2011-0126

## Silicon Carbide Phononic Crystals for Communication, Sensing, and Energy Management

**Maryam Ziaei-Moavved<sup>1</sup>, Charles Reinke<sup>1</sup>, Mehmet Su<sup>2</sup>, Ihab El-Kady<sup>1</sup>, and Roy H. Olsson III<sup>1</sup>**

<sup>1</sup> Sandia National Laboratories, Albuquerque, NM, USA

<sup>2</sup> Department of Electrical and Computer of Engineering, University of New Mexico, NM, USA  
mziaeim@sandia.gov, creink@sandia.gov, mfatihsu@ece.unm.edu, ielkday@sandia.gov, rholsso@sandia.gov

**Abstract:** We demonstrate design, fabrication, and characterization of silicon carbide phononic crystals used to confine energy in lateral overtone cavities in 2-3GHz range with high  $f.Q$  products in air. The SiC cavities are fabricated in a CMOS-compatible process with applications in communication systems, sensing, and thermal energy management.

Phononic crystals (PnC) have recently gained much attention due to their ability to precisely control and manipulate propagation of acoustic waves for applications in wireless communication, sensing, acoustic isolation, imaging, and thermal energy management. By strategically placing defects in the phononic crystal through removal or distortion of inclusions, cavities and waveguides have been demonstrated at RF frequencies [1-3]. Microfabricated phononic crystal cavity resonators provide a lower power small-footprint, CMOS-compatible alternative to discrete components in communication systems. Silicon carbide (SiC) due to its mechanical strength, high acoustic velocity, and low intrinsic material damping is a desirable structural material with applications from high temperature microelectronics to micromechanical oscillators and harsh environment sensors [4]. This paper describes the design, optimization, fabrication, and characterization of SiC PnC-based devices. Figure 1 shows a schematic of a SiC Fabry-Perot cavity suspended above the substrate with SiC/air PnCs as high reflectivity acoustic mirrors on each side of the cavity. Aluminum Nitride (AlN) transducers with interdigitated Al top electrodes are designed to excite and sense the acoustic resonances in the cavity. This device combines the benefit of piezoelectric transduction, while storing the acoustic energy in a low loss material resulting in high  $f.Q$  and  $k_r^2.Q$  products for oscillator and filter applications.

Opening a phononic bandgap requires proper selection of inclusion and matrix materials that yield the desired mismatch between the acoustic impedance and velocity. We will compare solid-air and solid-solid SiC phononic crystals using plane approximation method to understand the behaviour of the PnC bandgap. A typical dispersion diagram of elastic waves in a SiC/air phononic crystal with normalized inclusion radii  $r/a$  ranging from 0.35 to 0.5 and normalized slab thicknesses  $t/a$  from 0.25 to 5 is shown in Fig.2 (a), exhibiting a complete bandgap about 2.7GHz. Figure 2(b) shows simulated normalized transmission versus frequency and volume filling fraction,  $r/a$ , for a 7 period, cubic lattice of vacuum inclusions in SiC plate. As the filling fraction is increased, the bandgap width and depth increases while moving to lower frequencies.

The SiC cavities were fabricated in a six mask CMOS-compatible surface micromachining process [3]. The highly-textured cubic SiC film is deposited in a low pressure chemical vapor deposition system and optimized to have low stress and low surface roughness for high quality factor. Figure 3(a) shows a SEM of a 10<sup>th</sup> overtone SiC cavity separated from the AlN transducers by 5 layers of cubic SiC/Air PnC acoustic mirrors. Figure 3(b) shows a close-up SEM of the PnC with a lattice constant of 1.8 $\mu$ m and a filling fraction of 0.44. Figure 3(c) shows a close up view of one of the air holes etched in SiC with a nearly vertical sidewall (sidewall angle <5 $^\circ$ ). The SiC cavity resonators with frequencies ranging from 2 to 3GHz were tested in air using direct two-port transmission measurements. Aluminum nitride piezoelectric transducers were used to excite and detect the overtone acoustic cavities with frequencies ranging from 2 to 3GHz. Figure 4(a) shows the normalized transmission response of a 10<sup>th</sup> overtone cavity (cavity length=19.8 $\mu$ m) with 5 PnC layers at 2.24GHz with a quality factor of 2000. Figures 4(b) shows the normalized transmission response for a 50<sup>th</sup> overtone cavity (cavity length=99 $\mu$ m) with 3 PnC layers resulting in two resonant peaks with quality factors of 500 and 1000. The quality factors are improved to ~2200 and 3500 respectively by using 5 PnC layers (Fig.5(c)). These PnC-based cavities can be used to construct highly efficient acoustic signal processing elements such as filters and waveguides. These resonators are ideal for on-chip multi-frequency multi-bandwidth filter banks, on-chip spectrum analyzers, low phase noise oscillators, and ultra sensitive chemical and biological sensors. Furthermore, phononic crystals can be used in thermal energy management by shaping thermal phonon distribution resulting in reduced thermal conductivities [5]. Silicon carbide phononic crystal thermoelectric devices have a wide range of applications such as harsh environment microelectronics, thermoelectric energy generation, and satellite communication systems.

Phononics 2011: First International Conference on Phononic Crystals, Metamaterials and Optomechanics

Santa Fe, New Mexico, USA, May 29-June 2, 2011

PHONONICS-2011-0126

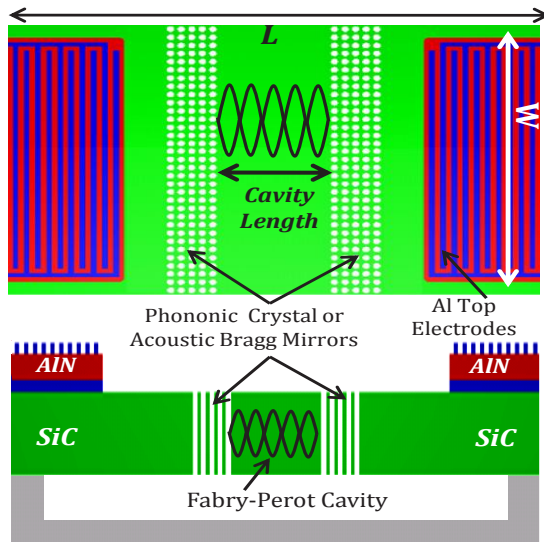


**Figure 1** Schematic of a SiC overtone phononic crystal cavity with 5 layer phononic crystals on each side of the cavity. The acoustic mirrors separate the cavity from the AIN piezoelectric transducers.

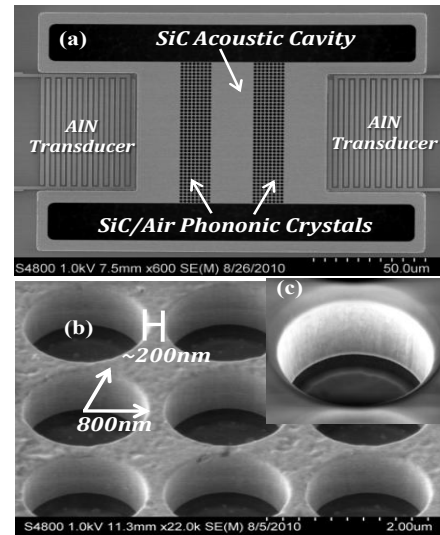


**Figure 3** (a) SEM of a fabricated silicon carbide 10<sup>th</sup> overtone cavity with drive/sense AIN transducers and 5 layers of PnC (b) close-up SEM of the SiC/air PnC with a 1.83µm pitch and filling fraction of 0.44 (c) SEM of one of the holes with vertical sides walls.

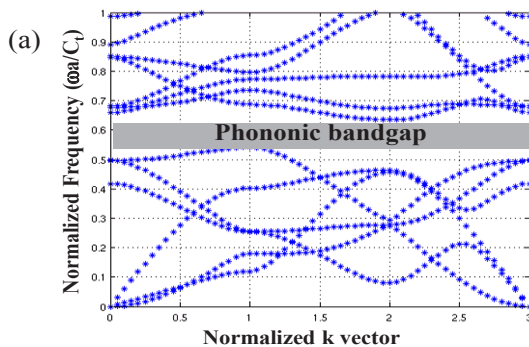


**Figure 2** (a) Acoustic band diagram of a 2D simple cubic SiC/air phononic crystal obtained from PWE simulations with  $r/a=0.45$  and  $t/a=0.5$ . (b) Simulated FDTD normalized transmission vs. frequency for a 7 layer cubic lattice of vacuum inclusions embedded in an infinitely thick SiC plate vs. inclusion filling fraction,  $r/a$ . The lattice constant,  $a$ , is 1.8µm.

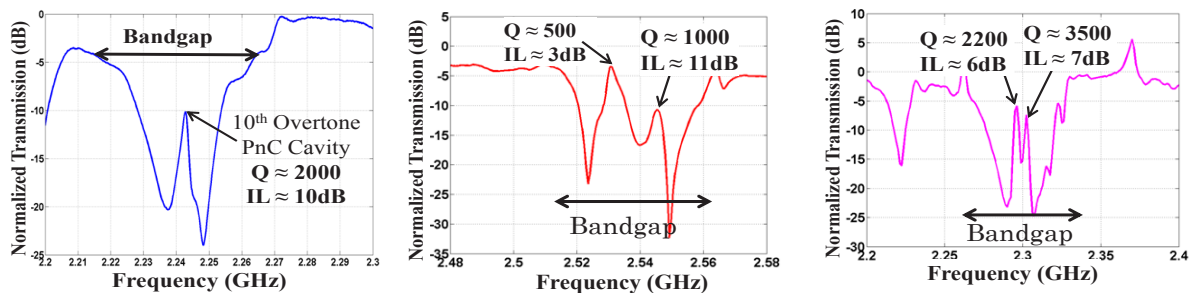
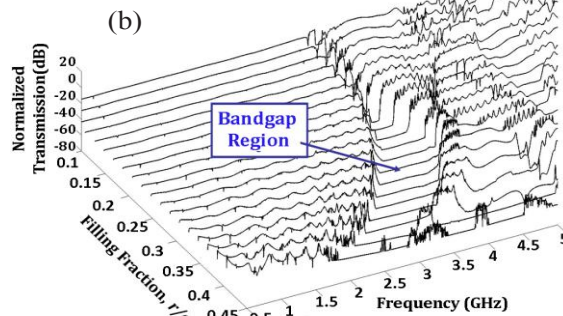


**Figure 4** Normalized transmission response of (a) 10<sup>th</sup> overtone cavity with 5 PnC layers and Q of ~2000 at 2.24GHz (b) 50<sup>th</sup> overtone cavity with 3 PnC layers and Q's of 500 and 1000 at 2.53 and 2.55GHz respectively (c) 50<sup>th</sup> overtone cavity with 5 PnC layers and Q's of 2200 and 3500 at 2.295 and 2.305GHz respectively.

## References

- <sup>1</sup>R. H. Olsson III, I. F. El-Kady, M. F. Su, M. R. Tuck, and J. G. Fleming *Sensors Actuators A*, **145–146**, pp. 87–93 (2008).
- <sup>2</sup>S. Mohammadi, A. A. Eftekhar, A. Khelif, H. Moubchir, W. D. Hunt, and A. Adibi, *Appl. Phys. Lett.*, **95**, 051906 (2009).
- <sup>3</sup>M. Ziaei-Moayyed, M. Su, C. Reinke, I. El-Kady, and R. Olsson III, *IEEE Ultrasonics Symposium 2010*, in press.
- <sup>4</sup>Y. T. Yang, K. L. Ekinci, K.L. M. H. Huang, L. M. Schiavone, M. L. Roukes, C. A. Zorman, and M. Mehregany *App. Phys. Lett.*, **78**, 162-164 (2001).
- <sup>5</sup>P.E. Hopkins, C. M. Reinke, M. F. Su, R. H. Olsson III, E. A. Shaner, Z. C. Lesemma, J.R. Serrano, L. M. Phinney, and I. El-kady, *Nano Lett.*, **11**, 107-112 (2010).

Phononics 2011: First International Conference on Phononic Crystals, Metamaterials and Optomechanics

Santa Fe, New Mexico, USA, May 29-June 2, 2011

PHONONICS-2011-0169

## Designing High-Q Compact Phononic Crystal Resonators

**Mehmet F. Su<sup>1</sup>, Drew F. Goettler<sup>1</sup>, Zayd C. Leseman<sup>1</sup>, Ihab El-Kady<sup>1,2</sup>**

<sup>1</sup> *Department of Mechanical Engineering, University of New Mexico, Albuquerque, NM, USA*  
mfatihsu@unm.edu, goettled@unm.edu, zleseman@unm.edu

<sup>2</sup> *Photonics Microsystems Department, Sandia National Laboratories, Albuquerque, NM, USA*  
ielkady@sandia.gov

**Abstract:** Phononic crystals provide a promising method of producing resonators with very high quality factors up to the theoretical limit possible in the host material. In this study we consider Silicon based solid-solid phononic crystal resonator designs with different lattices (simple cubic, hexagonal/triangular and honeycomb), number of inclusions and cavity shapes.

Compact microresonators are a versatile class of components used in both active such as oscillators and passive devices such as filters. One crucial requirement of any resonator device is a high quality factor, resulting in highly selective and tunable devices. Phononic crystals with cavity defects provide a method of producing compact resonators with quality factors reaching the maximum achievable figure for the constituent materials<sup>1</sup>. This talk will discuss our experiences in designing such resonators and optimizing the quality factor.

Phononic crystals consist of commonly cylinder shaped inclusions periodically placed in a host material (matrix). This study considered 2-D phononic crystals made of Tungsten inclusions in a Silicon matrix, placed in a number of lattice formations (simple cubic, hexagonal/triangular and honeycomb). The material pair was selected due to the large gap widths realizable using modest rod radius-to lattice periodicity ratios around 0.3. Low rod radius-to lattice periodicity ratios are more amenable to miniaturization, thus allowing smaller periodicities and higher operating frequencies<sup>2</sup> for phononic crystal resonators.

Numerical simulations were performed using the Finite Difference Time Domain (FDTD) method<sup>3</sup>. The FDTD numerical grid was terminated by Mur absorbing boundary conditions<sup>4</sup> in the designated primary propagation direction and periodic boundary conditions in the two transverse directions. This arrangement creates structures in infinite extent in the transverse while suppressing spurious reflections from the edges of the numerical grid. A wideband longitudinal displacement pulse was used to bootstrap all simulations. Postprocessing of the FDTD results for the frequency domain response was performed with Fourier Transform and Filter Diagonalization Method<sup>5</sup>. Resonator quality factors were calculated after obtaining the frequency domain response in each study case.

The resonator cavity was created by displacing half of the inclusions in the propagation direction, effectively forming a cavity extending infinitely along the transverse direction. This arrangement allows one to study wave penetration into the phononic crystal to develop an approximation in the form of a solid block, thus simplifying calculations for resonators and comparison to other types of reflectors. Isolated, periodically repeating cavities were also considered. Cavity frequencies and phononic crystal gaps in this study were optimized for an operating frequency of 1.315 GHz. Cavities supporting from the first up to the seventh harmonic were studied, all operating at the aforementioned frequency, to understand how the Q factor changes for various harmonic overtones and to determine the wave penetration into the phononic crystal. In this scheme, the fundamental frequency of the  $n$ th harmonic cavity is  $(1.315/n)$  GHz. If there was no wave penetration, the displacement for the  $n$ th harmonic cavity would be exactly  $n$  times the displacement needed for the first harmonic cavity. The presence of a constant wave penetration ( $\Delta$ ) into the tungsten inclusions requires accounting for both the wave penetration itself and another correction to the effective cavity length ( $L_{eff}$ ) due to the wave velocity difference between silicon and tungsten materials. This second correction factor is directly proportional to the wave velocity ratio between silicon and tungsten ( $c_{Si}/c_W$ ) and the wave penetration ( $\Delta$ ). Thus the effective cavity length for the  $n$ th harmonic cavity can be approximated as

$$L_{eff} = nL_1 + 2\Delta + (2n-2)(c_{Si}/c_W)\Delta \quad (1)$$

Phononics 2011: First International Conference on Phononic Crystals, Metamaterials and Optomechanics

Santa Fe, New Mexico, USA, May 29-June 2, 2011

PHONONICS-2011-0169

where  $L_1$  is the length for the first harmonic cavity,  $c_{Si}$  is the longitudinal wave velocity in silicon and  $c_W$  is the longitudinal wave velocity in tungsten. It is possible to solve for  $\Delta$  by determining  $L_1$  and the cavity length for any other harmonic for a predetermined operating frequency. Once  $\Delta$  is known, it becomes trivial to estimate the lengths of cavities supporting other harmonics.

The results indicate that the quality factors increase linearly with the cavity harmonic number and exponentially with the number of inclusions forming the phononic crystal reflectors. Clearly, the quality factor for a real resonator is limited by the fundamental material limit. For the studied cases, the limiting factor is the Akhieser effect<sup>6</sup> (phonon-phonon damping) loss. Incorporating the Akhieser effect into the quality factor calculation indicates phononic crystal resonators with as few as five layers of inclusions should attain the maximum quality factor possible in silicon material.

### References

- <sup>1</sup> D. Goettler, M. Su, Z. Leseman, Y. Soliman, R. H. Olsson III and I. El-Kady, *Journal of Applied Physics*, **108**, 084505 (2010).
- <sup>2</sup> M. F. Su, R. H. Olsson III, Z. C. Leseman and I. El-Kady, *Applied Physics Letters*, **96**, 053111 (2010).
- <sup>3</sup> M. M. Sigalas and N. Garcia, *Journal of Applied Physics*, **87**, 3122 (2000).
- <sup>4</sup> G. Mur, *IEEE Transactions on Electromagnetic Compatibility*, **23** (4), 377-382 (1981).
- <sup>5</sup> V. A. Mandelshtam and H. S. Taylor, *J. Chem. Phys.* **107** (17), 6756-6769 (1997).
- <sup>6</sup> T. O. Woodruff and H. Ehrenreich, *Phys. Rev.* **123**, 1553 (1961).

Phononics 2011: First International Conference on Phononic Crystals, Metamaterials and Optomechanics

Santa Fe, New Mexico, USA, May 29-June 2, 2011

PHONONICS-2011-0179

## A Waveguide-based Phononic Crystal Micro/Nano-mechanical High-Q Resonator

Saeed Mohammadi<sup>1</sup>, Ali A. Eftekhar<sup>1</sup>, Ali Adibi<sup>1</sup>

<sup>1</sup> School of Electrical and Computer Engineering, Georgia Institute of Technology, Atlanta, GA 30324, USA  
saeedm@gatech.edu, eftekhar@gatech.edu, adibi@ece.gatech.edu

**Abstract:** In this paper, we report the design, analysis, fabrication, and characterization of a very high frequency (VHF) phononic crystal (PnC) micro/nano-mechanical resonator architecture based on silicon (Si) PnC slab waveguides. Qs as high as 13,500 in air at a frequency of ~134 MHz with a motional resistance of ~600  $\Omega$ , and 35 dB spurious-free range of ~20 MHz are obtained.

Recently, PnC slab (plate) structures<sup>1</sup>, with large CPnBGs have been designed and implemented in platforms compatible with micro/nano-mechanical (MM) systems CMOS technologies<sup>2,3</sup>. The air (or vacuum) on top and bottom of a PnC slab (or membrane) decouples the vibrations in the PnC slab from leaking into the substrate. The possibility of realizing fundamental micro-mechanical (MM) devices, i.e., waveguides<sup>4,5</sup> and high quality factor (or high-Q) resonators<sup>6</sup>, which are the bases of integrated mechanical signal processing systems, have recently been demonstrated. Because of their unique properties, such PnC-based devices and systems may surpass their conventional silicon (Si) MM counterparts for a variety of applications including wireless communications and sensing.

In this paper, we introduce a new type of suspended MM resonators based on PnC slab waveguides that can effectively suppress the support loss using the CPnBG of the PnC, while providing mechanical support and a path to deliver electrical signal to interrogate the resonator. To eliminate the problem of spurious modes in the PnC slab resonators<sup>7</sup> and to prevent spurious interferences from other modes in the PnC structures, we start with the design of a PnC waveguide with a small number of modes. The PnC waveguide is then terminated by the PnC structure on its input and output to confine forward and backward (and hence standing) waves within the waveguide region to form a resonator.

The PnC structure studied in this paper is composed of a hexagonal (honeycomb) lattice of void cylindrical holes in a free-standing Si slab<sup>2</sup>. To form a PnC waveguide with small number of modes, we

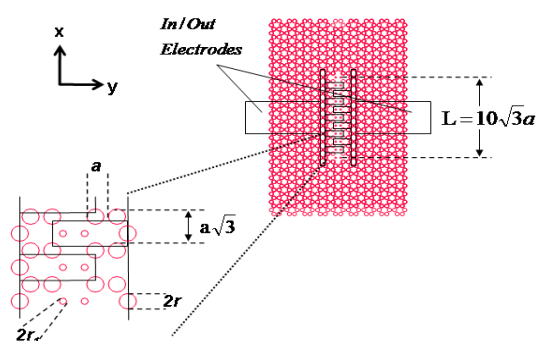


**Figure 1** Schematic of the layout of a waveguide-based PnC slab resonator structure with interdigital transducers placed on top of the cavity to excite and detect the modes of the resonator. The length of the cavity is approximately 10 periods ( $L = 10 a$ ).

reduce the radius of two lines of air holes in the PnC structure. A top-view schematic of such a PnC waveguide is shown in Fig. 1. The Extensional mode of the waveguide is utilized to allow for a more efficient excitation using the transducers and to obtain a high quality confinement. The radius of the immediate holes surrounding the waveguide are carefully chosen to be  $r' = 0.2a$ . In order to form the waveguide-based PnC resonator, the input and output ports of a waveguide are blocked by the PnC structure as shown in Fig. 1. The length of the confined waveguide is ten periods in the  $x$  direction ( $L = 10 a \sqrt{3}$ ).

The coupling of the resonator to/from the outside world is achieved by using piezoelectric transducers fabricated right on the PnC resonator. The number of PnC layers around the resonator in our design is 4 and 6 periods on each side of the cavity in the  $y$  and  $x$  direc-

tions, respectively, which are enough to almost completely eliminate leakage of acoustic energy from the sides of the resonator based on our previous observations<sup>6</sup>.

The waveguide-based resonator structure is fabricated with the scaling choice of  $a = d = 15 \mu\text{m}$  for the PnC structure. The fabrication process starts with a high-resistivity (to reduce electromagnetic coupling) silicon on insulator (SOI) wafer with a  $15\mu\text{m}$  device layer, a  $2\mu\text{m}$  buried oxide (BOX) layer

Phononics 2011: First International Conference on Phononic Crystals, Metamaterials and Optomechanics

Santa Fe, New Mexico, USA, May 29-June 2, 2011

PHONONICS-2011-0179

and a 400 $\mu\text{m}$  handle layer. A 100nm/1 $\mu\text{m}$ /100nm stack of Mo/AlN/Mo is sputtered on top of the device layer. The top Mo layer is patterned first using optical lithography and plasma etching to form the top electrode and contact pads. PnC holes are etched using a two-step plasma etching recipe to etch the transducer stack and the Si device layer. The access to the lower Mo electrode is obtained by selective wet etching of the AlN layer to the Mo layer. Finally, the structure is etched from the back using backside-alignment lithography and deep plasma etching of the handle and the BOX layers to release the structure and form the PnC slab resonator. A top view scanning electron microscope (SEM) image of the fabricated structure is shown in Fig. 2. The approximate geometrical parameters of the fabricated PnC resonator are measured to be  $a = 15 \mu\text{m}$ ,  $2r = 12.5 \mu\text{m}$  ( $r \sim 0.42a$ ), and  $2r' = 4.9 \mu\text{m}$  ( $r' \sim 0.16a$ ) using the

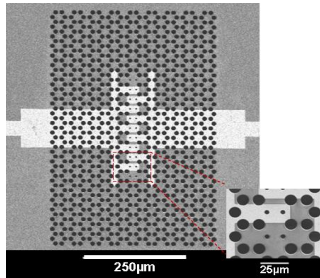


**Figure 2** An SEM image of the fabricated PnC resonator and a magnified version of a subset of this image (inset).

SEM data. The structure is characterized by using a two-port vector network analyzer with 50 $\Omega$  reference impedance to obtain the scattering parameters of the device in the PnBG frequency range.

In order to accurately evaluate the resonance properties of the main excited mode, we fitted a modified Butterworth Van Dyke (BVD) model<sup>8</sup> to the admittance profile of the desired mode. The fitted BVD model as well as the measured and fitted admittance and susceptance curves are shown in Figure 1, where  $C_p$  and  $R_p$  are the parallel capacitance and resistance between the upper and lower electrodes of the port, and  $R_r$ ,  $L_r$ , and  $R_m$  are associated with the electrical equivalent of the resonator at its resonance frequency, where the  $Q$  can be extracted from. As can be seen in this figure, the  $Q$  of the resonance is 13,500, which is by far the highest  $Q$  reported for PnC resonators<sup>6,9</sup> and significantly higher (>30 %)

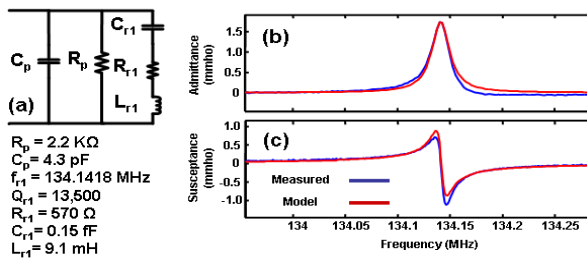


**Figure 1** (Color online) (a) The modified BVD model, (b) admittance, and (c) susceptance profile of the waveguide-based PnC resonator excluding the parasitic resistor and capacitor of the device. The frequency of resonance ( $f_{r1}$ ), the quality factor ( $Q_{r1}$ ), the motional resistance ( $R_r$ ), the resonance capacitance ( $C_{r1}$ ) and inductance ( $L_{r1}$ ) for the selected mode, and the values for the excluded parasitic capacitance and resistance ( $C_p$ ,  $R_p$ ) are given in this figure.

range of operation. This result confirms that obtaining high quality support-loss free MM resonators is possible through the use of the PnC structures.

This work was supported by the National Science Foundation (Contract No. 2106AXJ ARRA). The authors wish to thank the staff at Georgia Tech Nanotechnology Research Center for their support in holding the fabrication equipment, Prof. Reza Abdolvand for his input in fabrication, and Prof. W. D. Hunt for providing the measurement equipment.

## References

- <sup>1</sup> A. Khelif, B. Aoubiza, S. Mohammadi, A. Adibi, and V. Laude, *Physical Review E*, **74**, 46610-46615 (2006).
- <sup>2</sup> S. Mohammadi, A.A. Eftekhar, A. Khelif, H. Moubchir, R. Westafer, W.D. Hunt, and A. Adibi, *Electronics Letters*, **43**, 898-899 (2007).
- <sup>3</sup> S. Mohammadi, A.A. Eftekhar, A. Khelif, W.D. Hunt, and A. Adibi, *Applied Physics Letters*, **92**, 221903-221905 (2008).
- <sup>4</sup> S. Mohammadi, A.A. Eftekhar, W.D. Hunt, and A. Adibi, Piscataway, NJ, USA: IEEE, 768-772, (2008).
- <sup>5</sup> R.H. Olsson, I.F. El-Kady, M.F. Su, M.R. Tuck, and J.G. Fleming, *Sensors and Actuators A-Physical*, **145**, 87-93, (2008).
- <sup>6</sup> S. Mohammadi, A.A. Eftekhar, W.D. Hunt, and A. Adibi, *Applied Physics Letters*, **94**, 51903-51906 (2009).
- <sup>7</sup> S. Mohammadi, A. Eftekhar, A. Khelif, and A. Adibi, *Proc. of 2010 SPIE Photonics West*, 76090W, (2010).
- <sup>8</sup> K. S. Van Dyke, *Proceedings of the Institute of Radio Engineers*, **16** (6), 742-764, (1928).
- <sup>9</sup> C.-Y. Huang, J.-H. Sun, and T.-T. Wu, *Applied Physics Letters*, **97**, 031913 (2010).
- <sup>10</sup> B.P. Harrington and R. Abdolvand, *TRANSDUCERS 2009*, IEEE, 700-703 (2009).

